The parsec-scale structure of NGC 1275 at 1.3 GHz

G. B. Taylor[1] & R. C. Vermeulen
California Institute of Technology, Pasadena, CA 91125

ABSTRACT

We present a high dynamic range Very Long Baseline Array (VLBA) image of 3C 84 at 1.3 GHz. With these observations we have discovered a previously undetected component which is centered ∼65 mas to the south of the compact core, and has a diameter of ∼40 mas. The nucleus of 3C 84 thus displays radio emission without interruption from the core out to a total length of $0.1''$ (24 h^{-1} pc); clear evidence for activity of the central engine in the centuries preceding the latest large outburst in 1960. From the absence of significant emission to the north of the core we find that the free-free optical depth at 1.3 GHz is likely to be ≥ 3.7 at a projected distance of 3.5 h^{-1} pc.

Subject headings: galaxies:active — galaxies:individual(NGC 1275) — galaxies: jets — radio continuum: galaxies — galaxies:ISM — galaxies: nuclei

[1]Now at the National Radio Astronomy Observatory, Socorro, NM 87801

1. Introduction

The strong radio source 3C 84 (Perseus A) is associated with the nearby (z=0.0172) Seyfert galaxy NGC 1275. This galaxy is the dominant member of the Perseus Cluster. It is the closest example of a powerful core-dominated radio galaxy and therefore an object of frequent study, as well as a favorite calibrator source for radio observatories in the northern hemisphere. At z=0.0172, 1 mas = 0.24 h^{-1} pc, where $H_0 = 100\ h$ km s^{-1} Mpc^{-1}.

The radio emission of 3C 84 is detected on an unusually wide variety of angular scales. On the largest scale there is a halo of diameter $20'$ (300 h^{-1} kpc) associated with the Perseus cluster (Burns *et al.* 1992). Moving to smaller scales, Pedlar *et al.* (1990) find radio lobes extending $30''$ (7.2 h^{-1} kpc) in a position angle of 160°. Their VLA A-configuration image at 1.4 GHz shows an unresolved core component and a bright knot $4''$ (1 h^{-1} kpc) to the south, with fainter emission further out on both sides of the core. In VLBI observations the VLA core component is resolved into a number of bright, compact features, and a broad southern jet (Preuss *et al.* 1979; Unwin *et al.* 1982; Readhead *et al.* 1983; Romney *et al.* 1984; Marr *et al.* 1989; Venturi *et al.* 1993). Recent high dynamic range observations by Vermeulen, Readhead & Backer (1994) and by Walker, Romney & Benson (1994) revealed a weak counterjet 6 mas to the north of the core. Nearly-simultaneous VLBA observations from 5 to 43 GHz show that the counterjet exhibits a strong low-frequency cutoff (Romney *et al.* 1995), probably due to free-free absorption.

We observed 3C 84 for purposes of bandpass calibration, but upon imaging this source a heretofore unseen extension was discovered 55 mas (13 h^{-1} pc) to the south of the peak. That discovery motivated this letter.

2. Observations and Data Reduction

The observations were carried out at 1.347 GHz using the 10 element VLBA of the NRAO[2] on 1995 March 17-18. Seven scans, each of 13 minutes duration, were obtained on 3C 84. Both right and left circular polarizations were recorded using 2 bit sampling across a total bandwidth of 8 MHz. The VLBA correlator produced 512 frequency channels in each 4 second integration. Following correlation, global fringe fitting was performed using the AIPS task FRING, an implementation of the Schwab & Cotton (1983) algorithm. The fringe fitting was performed using a solution interval of 6.5 minutes and with the assumption of a point source model. Once delay and rate solutions had been applied the data were averaged in frequency over 8 MHz.

Amplitude calibration for each antenna was derived from measurements of the antenna gain and system temperature during each run. In addition, the strong calibrator DA193 (0552+398) was observed to refine the amplitude calibration. All editing, imaging, deconvolution, and self-calibration were performed using DIFMAP (Shepherd, Pearson & Taylor 1994, 1995). The two hands of polarization were added together for imaging, but were left separate in the self-calibration. Many iterations of phase self-calibration and imaging were performed before any attempt at amplitude self-calibration. At each iteration, windows for clean components were added, if necessary, to provide support and reject sidelobes. Convergence of the amplitude and phase solutions for this strong and complex source was much slower than for a typical source. The final naturally weighted image (Fig. 1) has a dynamic range of 10000 to 1. The rms noise in the image is 1.3 mJy/beam, which is still a factor of nearly 10 above the expected thermal noise. This discrepancy is primarily due to the combination of complicated source structure and comparatively poor u-v coverage.

In order to obtain quantitative information about the sizes and flux densities of the various components we performed Gaussian modelfitting to the self-calibrated data.

3. Discussion

The structure of 3C 84 shown in Fig. 1 can be characterized by 3 main components. The strongest component (S1) is resolved in the north-south direction with a size of 9.5 mas (Fig. 1). This component contains 21.2 Jy of the total flux density of 22.5 Jy (94%) at 1.3 GHz. On account of its extent and strength, we believe this component corresponds to the complex southern lobe-like component seen at higher frequencies (Readhead *et al.* 1983). The integrated spectral index of this component between 8.4 GHz (Walker *et al.* 1994) and 1.3 GHz is then $\alpha = -0.2$, where

[2] The National Radio Astronomy Observatory is operated by Associated Universities, Inc., under cooperative agreement with the National Science Foundation

$S \propto \nu^{\alpha}$. Without being able to derive quantitative information we can still estimate from the equal resolution images of Romney *et al.* (1995) that the spectral index is steeper between 8.4 and 5 GHz suggesting that the frequency of peak emission is between 1.3 and 5 GHz for S1. Assuming a single component in equipartition conditions (Scott & Readhead 1977), the turnover in the spectrum of S1 due to synchrotron self-absorption is predicted to occur at 1.1 GHz. Given that this component is known to contain complex substructure, the observed turnover is still consistent with synchrotron self-absorption. The turnover in the spectrum may have moved to lower frequencies since the analysis of earlier data (Unwin *et al.* 1982; O'Dea, Dent & Balonek 1984; Readhead *et al.* 1983).

The core component (C) is located at the northern end of S1. Its flux density is difficult to determine due to the proximity of S1, but our image is compatible with a flux density of 0.6 Jy as predicted from an extrapolation of the self-absorbed high-frequency spectrum (Romney *et al.* 1995). The northern counterjet (N1) recently discovered jointly by Vermeulen *et al.* (1994) and by Walker *et al.* (1994) has an even more inverted spectrum and, as predicted, is too faint to be discerned here.

A second extended component (S2) with diameter of $\sim$18 mas, located $\sim$19 mas (4.6 h^{-1} pc) to the south of S1, is consistent with the extended emission recently found at 5 GHz (Romney *et al.* 1995) and with the overall extent at 609 MHz derived from a simple modelfit (Wilkinson *et al.* 1979). We measure a flux density of component S2 at 1.3 GHz of 0.61 Jy. Assuming equipartition, the synchrotron self-absorption turnover frequency for S2 is 600 MHz, consistent with the findings of Wilkinson *et al.* (1979).

We have also discovered a further, previously unknown, southern component (S3) which is centered 55 mas (13 h^{-1} pc) to the south of S1, has a diameter of $\sim$40 mas, and has a flux density of 0.57 Jy. Assuming equipartition conditions, and a spectral index at high frequencies of $\alpha = -0.75$, component S3 should have a turnover frequency of 170 MHz. In fact, Sijbring (1993) predicted the presence of such a large component in order to explain observations of the low frequency spectrum of the nucleus of 3C 84. Prior VLBI observations of this well-studied source, such as those at 1.7 GHz by Biretta, Bartel & Deng (1991), have lacked the proper combination of low observing frequency, short baselines, and high dynamic range needed to detect this component.

The projected opening angle of the jet is $\sim 26°$ and it appears to be fairly constant with distance. The pc-scale structure of 3C 84 has the appearance of a broadening staircase. At the southern edge of both components S1 and S2 there is a clear step down in flux density. One possible explanation for these steps is that the emission was formed in successive bursts, each of which has been steadily expanding away from the central engine. Assuming a velocity of 0.34 mas yr^{-1} (Romney *et al.* 1995), the ages for S2 and S3 are 120 and 320 years, respectively. The component motions, however, may not be so equal. Marr *et al.* (1989) measured a velocity of 0.58 mas yr^{-1} for a fast-moving knot within our component S1.

It is likely that the emergence of component S1 was associated with the steady increase in the flux density of 3C 84 seen at cm wavelengths (e.g. Pauliny-Toth *et al.* 1976). This increase began shortly before regular flux-density monitoring commenced in the early 1960s (Kellermann & Pauliny-Toth 1968) and lasted through the mid-1980s (Preuss *et al.* 1979; Dent *et al.* 1983; O'Dea *et al.* 1984; Aller *et al.* 1985; Nesterov, Lyuty & Valtaoja 1995). If all three components were ejected from the nucleus in a single outburst 35 years ago, then the average angular motions derived from the leading edges of components S2 and S3 are 1.1 and 3.3 mas yr^{-1}, respectively. The leading edge velocity for S3 would need to be superluminal at 2.7 $h^{-1}c$. We consider this possibility unlikely given the lack of other evidence for highly relativistic motion in 3C 84.

The total flux density of 3C 84 at 1.3 GHz is completely dominated by component S1, which has been declining since the mid-1980s. If this were due to an unrestricted adiabatic expansion, then the flux density should have fallen as $S \propto t^{-2\gamma}$, where t is the time since becoming optically thin, and $\gamma = 1 - 2\alpha$ (Kellermann & Pauliny-Toth 1968). However, the flux density is dropping only by of order 10 % per year, much less rapidly than predicted for any reasonable spectral index. Furthermore, assuming that S1, S2 and S3 were produced in successive bursts of the same strength that became optically thin after the same interval ($\sim$25 yr), and that the distance from the core is proportional to age, then this sequence of features is inconsistent with free expansion; in particular S3 is more than an order of magnitude too bright for this scenario. It is possible that the steps in brightness which help to define S1, S2 and S3 are, at least in part, the result of changes in the density of the external medium. Changes in external density could lead to discontinuous expansion episodes, the formation of shocks, and particle re-acceleration. In fact S1, S2, and S3 may not be strictly the products of discrete flaring events, but rather they may result from semi-continuous (but variable) activity in the core over the last several hundred years.

The recently discovered counterjet component N1 has a low-frequency cutoff, probably because it is on the far side of a free-free absorbing disk surrounding the center of activity (Levinson, Laor, & Vermeulen 1995). The jet-to-counterjet ratio for the integrated brightnesses of N1 and S1 is 9 at 22 GHz, where the free-free opacity is low (Vermeulen *et al.* 1994). Assuming that this jet-to-counterjet ratio is due to Doppler beaming, and that at 22 GHz optically thin synchrotron radiation is observed from both sides, then this ratio of 9 is an upper limit to the ratio which would be observed at lower frequencies in the absence of obscuring material. The reason this is an upper limit is because the spectral index of the emission at 1.3 GHz is flatter than at 22 GHz, and therefore the effects of Doppler boosting are lessened. We might therefore expect to see counterparts to components S2 and S3 with peak flux densities at 1.3 GHz of $\geq$50 and $\geq$4 mJy/beam respectively. The counterpart (N2) to S2 would thus be at $\geq$40 times the noise level in Fig. 1. Using the arm length ratio of 2:1 between S1 and N1 seen at high frequency (Vermeulen *et al.* 1994), we conclude that at the predicted projected distance of N2, 3.5 h^{-1} pc, the free-free optical depth at 1.3 GHz is $\tau_{1.3} \geq 3.7$. With an expected peak of 4 mJy/beam the counterpart to S3 would only appear at the 3 σ level. We have made the tapered image shown in Fig. 2 to obtain increased sensitivity to weak extended emission. While there is marginal evidence for emission near the predicted location of N3, the result is inconclusive. Going to still larger scales, Pedlar *et al.* (1990) find a peak of 50 mJy at a projected distance of 1 h^{-1} kpc south of the core. No counterpart to this component is seen to the north, but the expected flux density is only $\sim$6 mJy, or 4 times the noise in their image. On still larger scales (5–10 kpc) the lobes of 3C 84 are quite symmetric.

4. Conclusions

We present the first observation of an extended feature located 65 mas to the south of the core of 3C 84. From this we reason that the nucleus has been active, at least semi-continuously, for the past few centuries. The flux densities and spectra of the three main components visible at 1.3 GHz are not compatible with unimpeded adiabatic expansion, but require a more complex external density distribution and/or the occurrence of particle re-acceleration in shocks. The absence of a counterjet indicates that the optical depth due to free-free absorption exceeds 3.7 out to a projected distance north of the core of at least 3.5 h^{-1} pc.

High sensitivity VLBI observations at lower frequencies are in progress to determine the extent of 3C 84 to the south on the pc-scale, and to search for the presence of a northern counterjet.

The authors thank the referee, Jonathan Marr, for helpful comments on the manuscript. This research has made use of the NASA/IPAC Extragalactic Database (NED) which is operated by the Jet Propulsion Laboratory, Caltech, under contract with NASA. This work was supported by the NSF under grant AST-9420018.

REFERENCES

Aller, H. D., Aller, M. F., Latimer, G. E., & Hodge, P. E. 1985, ApJS, 59, 513

Biretta, J. A., Bartel, N., & Deng, J. 1991, in IAU Colloq. 131, Radio Interferometry: Theory, Techniques, and Applications, ed. T. J. Cornwell & R. A. Perley (ASP Conf.Ser.19; San Francisco:ASP), 334

Burns, J. O., Sulkanen, M. E., Gisler, G. R., & Perley, R. A. 1992, ApJ, 388, L49

Dent, W. A., O'Dea, C. P., Balonek, T. J., Hobbs, R. W., & Howard, R. J. 1983, Nature, 306, 41

Kellermann, K. I., & Pauliny-Toth, I. I. K., 1968, ARA&A, 6, 417

Levinson, A., Laor, A., & Vermeulen, R. C. 1995, ApJ 448, 589

Marr, J. M., Backer, D. C., Wright, M. C. H., Readhead, A. C. S., & Moore, R. 1989, ApJ, 337, 671

Nesterov, N. S., Lyuty, V. M., & Valtaoja, E. 1995, A&A, 296, 628

O'Dea, C. P., Dent, W. A., & Balonek, T. J. 1984, ApJ, 278, 89

Pauliny-Toth, I. I. K., Preuss, E., Witzel, A., Kellermann, K. I., Shaffer, D. B., Purcell, G. H., Grove, G. W., Jones, D. L., *et al.* 1976, Nature, 259, 17

Pedlar, A., Ghataure, H. S., Davies, R. D., Harrison, B. A., Perley, R. A., Crane, P. C., & Unger, S. W. 1990, MNRAS, 246, 477

Preuss, E., Kellermann, K. I., Pauliny-Toth, I. I. K., Witzel, A., & Shaffer, D. B. 1979, A&A, 79, 268

Readhead, A. C. S., Hough, D. H., Ewing, M. S., Walker, R. C., & Romney, J. D. 1983, ApJ, 265, 107

Romney, J. D., Alef, W., Pauliny-Toth, I. I. K., Preuss, E., & Kellermann, K. I. 1984, in VLBI and Compact Radio Sources, IAU Symp. 110, eds. R. Fanti, K. I. Kellermann, & G. Setti (Dordrecht:Reidel), 137

Romney, J. D., Benson, J. M., Dhawan, V., Kellermann, K. I., Vermeulen, R. C., & Walker, R. C. 1995, PNAS, 92, in press

Scott, M. A., & Readhead, A. C. S. 1977, MNRAS, 180, 539

Schwab, F. R., & Cotton, W. D. 1983, AJ, 88, 688

Shepherd, M. C., Pearson, T. J., & Taylor, G. B. 1994, BAAS, 26, 987

Shepherd, M. C., Pearson, T. J., & Taylor, G. B. 1995, BAAS, 27, 903

Sijbring, L. G. 1993, PhD thesis, University of Groningen

Unwin, S. C., Mutel, R. L., Pillips, R. B., & Linfield, R. P. 1982, ApJ, 256, 83

Venturi, T., Readhead, A. C. S., Marr, J. M., & Backer, D. C. 1993, ApJ, 411, 552

Vermeulen, R. C., Readhead, A. C. S., & Backer, D. C. 1994, ApJ, 430, L41

Walker, R. C., Romney, J. D., & Benson, J. M. 1994, ApJ, 430, L45

Wilkinson, P. N., Readhead, A. C. S., Anderson, B., & Purcell, G. H. 1979, ApJ, 232, 365

This 2-column preprint was prepared with the AAS LaTeX macros v4.0.

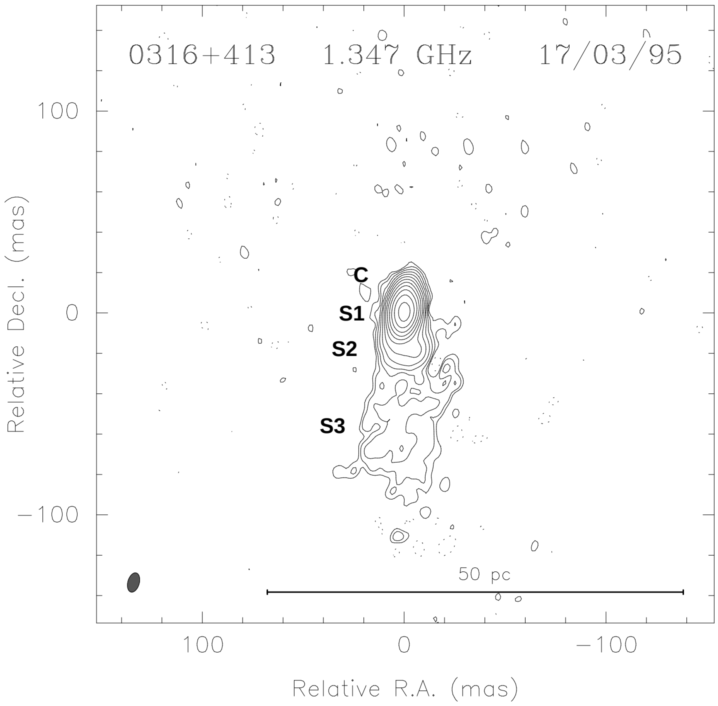

Fig. 1.— The naturally weighted image of 3C 84 at 1.347 GHz. The restoring beam has dimensions 9.8 × 5.7 mas in position angle $-16°$. Contour levels are at −4, 4, 8, 16, 32, ... 8192 mJy/beam with negative contours shown as dashed lines.

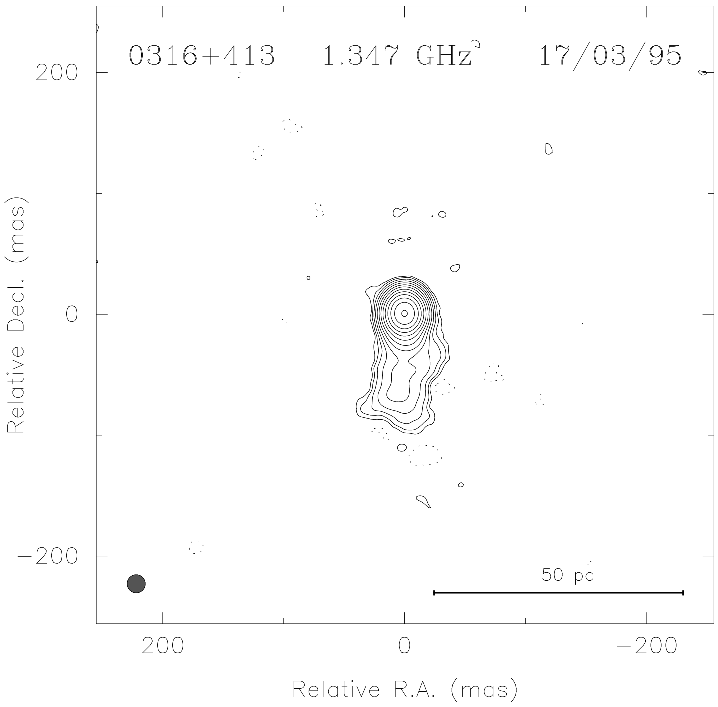

Fig. 2.— The naturally weighted and tapered image of 3C 84. A Gaussian taper falling to 50% at 10 Mλ was applied and the image was restored with a circular 15 mas beam. Contour levels are at −4, 4, 8, 16, 32, ... 16384 mJy/beam.